NUCL SCI TECH (2021) 32:74
https://doi.org/10.1007/s41365-021-00908-9

Impact of finite-range tensor terms in the Gogny force on the β-decay of magic nuclei

Da-Zhuang Chen[1] · Dong-Liang Fang[2,3] · Chun-Lin Bai[1]

Received: 15 April 2021 / Revised: 17 May 2021 / Accepted: 26 May 2021 / Published online: 16 July 2021

Abstract Effects of finite-range tensor force on β-decay of magic and semimagic nuclei of ^{34}Si, ^{68,78}Ni, and ^{132}Sn have been investigated using the self-consistent Hartree–Fock plus random-phase approximation model. The tensor force shifts the low-lying Gamow–Teller states downward and systematically improves the calculations of Q and $\log ft$ values. Consequently, it systematically reduces the deviations between the theoretical and experimental data and significantly improves the calculation of β-decay half-lives. This effect is similar to that of zero-range tensor force.

Keywords Finite-range tensor force · Gogny force · β -decay · Magic nuclei · Half-life · Q value · $\log ft$ value

1 Introduction

The null β^--decay half-lives of the very neutron-rich nuclei play an important role in the r-process nucleosynthesis, which governs the synthesis of nearly half of the elements heavier than iron [1–3]. The r-process occurs in neutron-rich sites and involves the continuous and rapid transfer of nuclei to the neutron-rich region through neutron capture, until the neutron capture rates become comparable to the ones of β^--decay. The β^--decay increases the proton number of neutron-rich nuclei and enables their conversion into heavier elements. The final abundance of any stable nuclei depends strongly on the competition between the β-decay and the neutron capture rates. Therefore, the β-decay half-life is an essential input for the r-process calculations.

As the r-process nuclei are in the neutron-rich area, most of them are beyond the scope of the current experiment; therefore, the r-process calculations must rely on theoretical estimations. Various theoretical models have been developed for this purpose. Basically, the various β -decays can be understood by utilizing the time-dependent perturbation theory [4]. Macroscopic gross theory, which adopts the sum rules of the β -decay strength function as well as the single particle energy distribution, can estimate the β-decay half-lives for the entire nuclide chart [5, 6]. Among the most well-known microscopic approaches, the nuclear shell-model includes all the correlations consistently and accurately reproduces the experimental β-decay half-lives of the waiting-point nuclei at $N = 50$ [7], 82 [8, 9], and 126 [10]. Furthermore, the roles played by Gamow–Teller and first-forbidden transitions have also been investigated in the large-scale shell model calculations [11]. However, their applicability is limited to medium–heavy nuclei or those localized around magic numbers, owing to their large configuration space. Another useful microscopic approach is the proton–neutron quasi-particle random-phase approximation (pn-QRPA) [12–14]. pn-QRPA

This work was supported by the National Natural Science Foundation of China (Nos. 11575120 and 11822504) and the Science Specialty Program of Sichuan University (No. 2020SCUNL210).

✉ Chun-Lin Bai
bclphy@scu.edu.cn

1 College of Physics, Sichuan University, Chengdu 610065, China

2 Institute of Modern Physics, Chinese Academy of Sciences, Lanzhou 730000, China

3 University of Chinese Academy of Sciences, Beijing 100049, China

models can be used for global calculations, which are based on realistic nucleon–nucleon interactions [15–17] or effective interactions such as the relativistic interaction [18–20], non-relativistic zero-range Skyrme interaction [21–23], and finite-range Gogny interaction [24]. In the QRPA calculations, the isoscalar pairing interaction [18, 21] and the tensor interaction [22] were shown to provide strong impact on the low-lying excited states and subsequently the β-decay half-life.

Inspired by the shell model calculations performed to determine the role played by the tensor force in elucidating the new magic numbers in the exotic neutron-rich nuclei [25–27], significant attention has been paid to the role played by the tensor terms (especially the zero-range one) in nuclear many-body calculations. These studies show that zero-range tensor interactions can improve the description of ground-state properties, such as single-particle energies [28, 29], shell evolutions [30, 31], binding energies [32, 33] and the stability of superheavy nuclei [34, 35]. Moreover, such terms also strongly impact the collective excitations associated with the non-charge exchange [36–38] and the spin–isospin excitations associated with charge–exchange, such as the Gamow–Teller (GT) transitions [39, 40], spin-dipole transitions [41–43], and the β-decay half-life [22]. After noticing the above effects induced by the zero-range tensor interactions in the non-relativistic calculations, such effects were also investigated in the relativistic density functional calculations by separating out tensor force components; these studies show improvements in the descriptions of ground-state properties derived from tensor force [44–46]. However, for the QRPA calculations based on the relativistic mean field (in which the tensor interaction was not included due to the exclusion of the Fock term), the effects of tensor force on the spin–isospin excitations [47] and β-decay half-life were not observed [18, 20]. When the tensor force was taken into account by including the Fock term, the effect of the tensor force on the GT transition was still negligible [48, 49]. Meanwhile, studies on finite-range tensor terms have also been performed using Gogny interactions to elucidate the exotic neutron-rich nuclei. These studies have shown that the inclusion of the tensor force improves the single-particle energies [50–52] and collective spin–isospin excitation energies [53, 54]; however, the effect of the tensor force on the β-decay half-life has not been studied so far.

In this work, the HF + RPA model based on Gogny force has been applied to study the impact of the finite-range tensor terms on the β-decay of magic and semimagic nuclei of (^{34}Si, ^{68,78}Ni and ^{132}Sn). The aim was to determine whether the finite-range tensor force can improve the β-decay half-life; this has been reported previously in the DFT + QRPA model that is based on the zero-range tensor force; however, this result has not been obtained using the RMF + QRPA model.

The remainder of this paper is organized as follows: In Sect. 2, we briefly present the HF + RPA model and the β-decay theory. In Sect. 3, some details of the HF + RPA calculations as well as parameters of the Gogny interactions including finite-range tensor terms are provided. In Sect. 4, the β^--decay half-lives and the Q and $\log ft$ values are predicted, analyzed, and compared to the experimental data. The conclusions are given in Sect. 5.

2 Formulism and method

The β-decay of the presently studied nuclei in this work is dominated by the GT transition, in which the transition operator is defined as:

$$O^{\mathrm{GT}\pm} = \sum_{i=1}^{A} t_{\pm}^{i}\sigma^{i}, \tag{1}$$

where the isospin operator, $t_{\pm} = \frac{1}{2}(t_x + it_y)$. In the RPA model, the creation operator for these collective excited states can be expressed as:

$$Q_{J^\pi M}^{m\dagger} = \sum_{qk}\left[X_{qk}^{m}\mathcal{A}_{qk,J^\pi M}^{\dagger} - Y_{qk}^{m}\tilde{\mathcal{A}}_{qk,J^\pi M}\right], \tag{2}$$

where the coherent coefficients X and Y denote the forward and backward amplitudes, respectively, which may be obtained by solving the RPA equation.

$$\mathcal{A}_{qk,J^\pi M}^{\dagger} \equiv [a_q^{\dagger}a_k]_{J^\pi M}$$

In the above formula, $a^{\dagger}$ and a represent the standard single-particle creation and annihilation operators, respectively. Meanwhile, J and π denote the total angular momentum and parity, respectively, for the transitions.

After diagonalizing the RPA equation, we can obtain the GT strength:

$$B_{1_m^+}^{\mathrm{GT}\pm}(\omega_m) = |\langle 1_m^+||O^{\mathrm{GT}\pm}||0\rangle|^2, \tag{3}$$

where ω_m is the excitation energy of the mth GT state with respect to the ground state of the mother nucleus.

Once the GT states have been obtained from the HF + RPA calculations, the GT-type β^--decay half-life can be calculated using the expression [21]:

$$T_{1/2} = \frac{D}{g_A^2\sum_m B_m^{\mathrm{GT}-} f_0(Z, A, \omega_m)}, \tag{4}$$

where $D = 6163.4 \pm 3.8$ s (e.g., see Ref. [55]), and the ratio of the axial-vector and vector coupling constants, $g_{\mathrm{A}} \equiv G_{\mathrm{A}}/G_{\mathrm{V}} = 1.26$, where G_{A} is the axial-vector coupling constant, G_{V} is the vector coupling constant. By assuming a quenching factor of 0.7 [56, 57], g_A was set at 0.882. Here, the sum runs over all 1^+ states within the β-decay energy window $Q = \Delta_{nH} - \omega_m > 0$ MeV, with $\Delta_{nH} = 0.78227$ MeV denoting the mass difference between the neutron and hydrogen atom.

The $\log ft_m$ value for each allowed state, which is related to the GT decay with $\Delta J^\pi = 1^+$, can be obtained [21]:

$$\log ft_m = \log_{10}\left(\frac{D}{g_A^2 B^{\mathrm{GT}-}_{1_m^+}}\right). \tag{5}$$

3 Details of the calculations

In this section, we provide details of the HF + RPA calculations and the parameters.

The HF equation has been solved using the spherical-harmonic oscillator basis expansion method with the main quantum number cutoff being set at $N\mathrm{max} =$ 6, 8, and 10 for ^{34}Si, ^{68,78}Ni, and ^{132}Sn, respectively. For each nucleus, the harmonic oscillator width $\hbar\omega$ has been chosen according to an interpolation formula [58]

$$\hbar\omega = (0.0002A^2 - 0.1A + 21.1)\,\mathrm{MeV}. \tag{6}$$

In our present RPA calculations, all the central and tensor terms have been included. The residual two-body spin–orbit interaction is excluded in the RPA, because the RPA correlations of the spin–orbit interaction produce a trivial effect on the GT transition. Furthermore, the self-consistency is well kept in the present HF + RPA model. The only input required by our self-consistent HF + RPA approach is the Gogny-like interactions that include tensor terms. The original Gogny interaction was proposed to exhibit the following form [59, 60]:

$$\begin{aligned} V_{\mathrm{eff}}(1,2) = {} & \sum_{i=1}^{2} \exp\left[\frac{-(\boldsymbol{r}_1 - \boldsymbol{r}_2)^2}{\mu_i^2}\right] \\ & \times (W_i + B_i\hat{P}_\sigma - H_i\hat{P}_\tau - M_i\hat{P}_\sigma\hat{P}_\tau) \\ & + iW_{LS}(\boldsymbol{\sigma}_1 + \boldsymbol{\sigma}_2)\cdot \overleftarrow{\nabla}_{12} \times \delta(\boldsymbol{r}_1 - \boldsymbol{r}_2)\overrightarrow{\nabla}_{12} \\ & + t_3(1 + x_0\hat{P}_\sigma)\delta(\boldsymbol{r}_1 - \boldsymbol{r}_2)\left[\rho\left(\frac{\boldsymbol{r}_1 + \boldsymbol{r}_2}{2}\right)\right]^\alpha \\ & + \left(\frac{1-\tau_{1z}}{2}\right)\left(\frac{1-\tau_{2z}}{2}\right)\frac{e^2}{|\boldsymbol{r}_1 - \boldsymbol{r}_2|}. \end{aligned} \tag{7}$$

It is composed of central and spin–orbit terms. The central interaction consists of two distinct Gaussians with ranges μ_1 and μ_2. $\hat{P}_\sigma$ and $\hat{P}_\tau$ denote the standard spin and isospin exchange operators, respectively.

Following the work of Refs. [50, 51, 61], we included the tensor terms of the Gaussian form:

$$\begin{aligned} V_{\mathrm{tensor}}(1,2) &= (V_{\mathrm{T1}} + V_{\mathrm{T2}}\hat{P}_\tau)\hat{S}_{12}\exp\left[-\frac{(\boldsymbol{r}_1 - \boldsymbol{r}_2)^2}{\mu_{\mathrm{T}}^2}\right] \\ &= \left[\left(V_{\mathrm{T1}} + \frac{1}{2}V_{\mathrm{T2}}\right) + \frac{1}{2}V_{\mathrm{T2}}\boldsymbol{\tau}_1\cdot\boldsymbol{\tau}_2\right] \\ &\quad \times \hat{S}_{12}\exp\left[-\frac{(\boldsymbol{r}_1 - \boldsymbol{r}_2)^2}{\mu_{\mathrm{T}}^2}\right], \end{aligned} \tag{8}$$

where μ_{T} corresponds to the longest range of the central terms, V_{T1} and V_{T2} are the two parameters, and $\hat{S}_{12}$ is the usual tensor operator [53].

We performed HF + RPA calculations with the well-known D1S [62] and D1M [63] interactions. All tensor parameters based on Eq. (8), including D1ST2a [50], D1ST2b [50], D1ST2c [51], D1MT2a [64], D1MT2c [54, 64], and D1MTd [52], were employed to calculate the relevant quantities (e.g., half-lives $t_{1/2}$, Q value, and $\log ft$) of ^{132}Sn, ^{68,78}Ni, and ^{34}Si. After the calculations, we found that compared to the standard D1S or D1M parameters, the above-mentioned parameters do not improve the description of the properties associated with β-decay of these nuclei and fail to reproduce the half-lives. Therefore, the tensor parameters must be tuned to accurately reproduce the β-decay properties of these nuclei.

Following the procedure adopted in Refs. [50, 51], we tune the values of V_{T1} and V_{T2} by reproducing the 8.8 MeV experimental splitting between the neutrons of the $1f_{7/2}$ and $1f_{5/2}$ states in ^{48}Ca [65], together with the experimental half-lives of doubly magic and semimagic nuclei. Using this procedure, two sets of parameters (D1STx and D1MTx) were obtained, as shown in Table 1. It should be noted that the tensor terms are just added perturbatively on top of the existing force, and the present strengths of the tensor terms are adjusted with only a few properties that are considered. For a wider global use, one needs to produce effective interactions with the tensor force by using a full variational procedure to fit the tensor and the central terms on equal footing; this procedure should take into account more quantities.

Table 1 Values of the tensor force parameters are defined in Eq. (8) for D1STx and D1MTx interactions

	V_{T1} (MeV)	V_{T2} (MeV)	μ_{T} (fm)
D1STx	− 155	75	1.2
D1MTx	− 210	160	1.0

The other parameters in the D1S and D1M forces remain unchanged

4 Results and discussion

In this section, we reveal the β-decay half-lives of doubly magic and semimagic nuclei of ^{132}Sn, ^{68,78}Ni, and ^{34}Si, as well as their Q and $\log ft$ values. We focus on the differences between the results calculated with and without the tensor force.

The β-decay half-lives of ^{34}Si, ^{68,78}Ni, and ^{132}Sn are shown in Fig. 1 and have been compared with experimental data [66, 67]. The half-lives calculated with D1S and D1STx are presented in panel (a), whereas those calculated with D1M and D1MTx are shown in panel (b). The arrows denote the infinite half-lives. The results calculated with D1S and D1M systematically overestimate the experimental data of ^{68}Ni, ^{34}Si, and ^{78}Ni, and fail to predict the β-decay of ^{132}Sn. However, when the tensor forces D1MTx and D1STx are included, the half-lives are reduced systematically, the calculations can predict the β-decay for ^{132}Sn, and other significant improvements can be observed. With D1MTx, the half-lives of ^{68}Ni, ^{34}Si, and ^{78}Ni are reduced and close to the experimental values; however, for ^{132}Sn, the half-life is still larger than its experimental counterpart. With D1STx, the half-lives of ^{68}Ni, ^{34}Si, and ^{78}Ni agree well with experimental data, and the half-life of ^{132}Sn was closer to the experimental value.

The β-decay Q values of the four nuclei, together with the experimental data, are displayed in Fig. 2 to understand the origin of this systematic reduction in the half-lives that is caused by the tensor force. In the figure, the Q values of the branches with the largest branching ratios are selected for comparison with the experimental Q values. The decay scheme of ^{78}Ni has not been identified experimentally; the

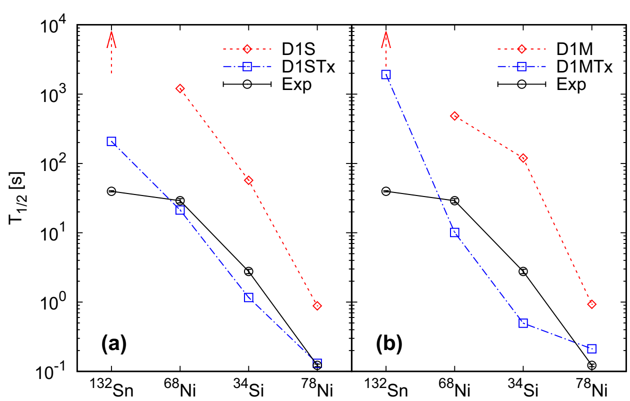

Fig. 1 (Color online) β-decay half-lives of ^{34}Si, ^{68,78}Ni, and ^{132}Sn obtained by performing calculations with D1S and D1STx (**a**), as well as D1M and D1MTx (**b**) interactions. The results calculated without the tensor force are labeled using red diamond-dashed lines, while those obtained with the tensor force are labeled using blue diamond-dash-dot lines. The experimental data have been obtained from Refs. [66, 67], which are labeled using black circle lines with error bars. The arrows denote infinite half-lives

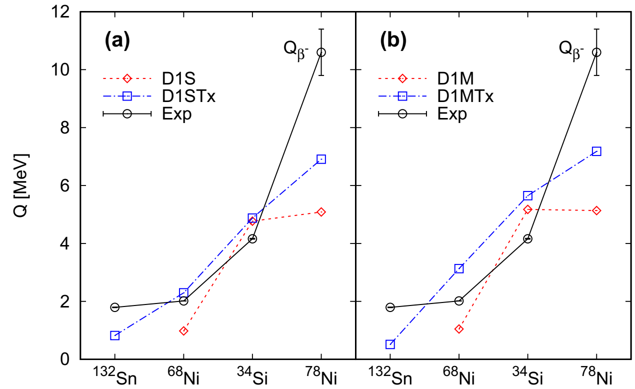

Fig. 2 (Color online) Same as Fig. 1, but for the Q values of the β-decay of ^{132}Sn, ^{68}Ni, ^{34}Si and ^{78}Ni

experimental Q_{β^-} value [66, 67] is shown instead in the panels. It can be seen that the Q values for the four nuclei are enhanced by the tensor force as it shifts the low-energy GT states downward. As observed in panel (a), with D1STx, the Q values for ^{68}Ni and ^{78}Ni increased by approximately 1 MeV; for ^{34}Si, the Q value is enhanced slightly. Meanwhile, for ^{132}Sn, β-decay becomes possible, although the theoretical Q value is underestimated. In general, with the inclusion of the tensor force, the Q values for ^{68}Ni and ^{34}Si can be accurately reproduced, while the Q value for ^{132}Sn is still approximately 1 MeV smaller than the experimental value. As observed in panel (b), with D1MTx, the Q values of ^{68,78}Ni are enhanced significantly; however, this increase is less significant for ^{34}Si.

Furthermore, the $\log ft$ values of the four nuclei, which are related to the GT strength of the decay with the largest branching ratio (Fig. 3), have been compared with the experimental data. As observed in panel (a), when the tensor force is absent, the $\log ft$ values of ^{68}Ni and ^{34}Si are

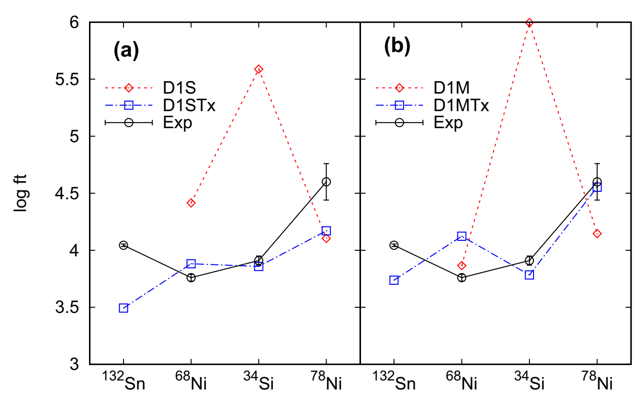

Fig. 3 (Color online) The same as Fig. 2, but for $\log ft$. The experimental data of $\log ft$ values of ^{132}Sn, ^{68}Ni, and ^{34}Si were taken from Refs. citeAudi,NNDC. The experimental reference value of $\log ft$ value for ^{78}Ni [66, 67] is evaluated from its experimental Q_{β^-} value

much larger than the experimental values. After the tensor force D1STx is included, the $\log ft$ values of ^{68}Ni and ^{34}Si are drastically reduced, which implies that the tensor force can shift the strength to the low-energy GT states and further shift these states downward to lower excitation energies. As observed in panel (b), with D1M and D1MTx, the $\log ft$ values are reasonably reproduced; however, for ^{34}Si, D1M tends to largely overestimate the experimental value.

Based on the above-mentioned results of the Q and $\log ft$ values, the effects of the tensor force on the β-decay half-life have been understood thoroughly. In ^{132}Sn, the tensor force shifts the low-energy GT state to an energy lower than the β-decay threshold; hence, β-decay is possible. However, the Q values obtained by D1STx and D1MTx are lower than the experimental values by approximately 1.2 and 1.6 MeV, respectively, while the calculated half-lives are still greater than their experimental values. In the case of ^{68}Ni, its half-life is accurately reproduced with D1STx as both the Q_{β^-} and $\log ft$ values are also reproduced well; however, with D1MTx, the half-life is underestimated slightly because the Q value is somewhat overestimated. In ^{34}Si, owing to the large $\log ft$ value (weak GT strength), the calculation performed without tensor force overestimates the half-life, whereas the inclusion of the tensor force circumvents this problem. In ^{78}Ni, as the tensor force enhances the Q value, the half-life is reproduced well.

5 Conclusion

In this study, we added a finite-range tensor force to the self-consistent HF + RPA model by employing the Gogny interaction to investigate the impact of the tensor force on the β-decay half-lives of magic and semimagic nuclei of ^{132}Sn, ^{68,78}Ni, and ^{34}Si. The tensor force was added on the existing Gogny interactions D1S and D1M, and two parameter sets were adopted: D1STx and D1MTx. Our calculations show that the β-decay half-live calculations for the four nuclei are significantly and systematically improved with the inclusion of the tensor force, which considerably reduces the half-lives by shifting the low-energy GT state downward and increasing the strength of these transitions. We also determine the Q and $\log ft$ values, which provide details of how the tensor force reduces the half-lives. These results suggest that the tensor force decreases half-lives naturally as calculations for both the Q and $\log ft$ values are improved. The global calculations of the β-decay half-lives, including the finite-range tensor force, need to be performed in future studies. This is because the present HF + RPA model is only valid for semimagic and magic nuclei, which are close to the shells and spherical in shape. Consequently, the pairing interaction and the quasi-particle approximation should be added to the open-shell nuclei, while the deformation effect should be included.

Moreover, this work, together with that of Ref. [22], shows that for both the non-relativistic effective Gogny and Skyrme interactions, the tensor force can reduce the β-decay half-lives; however, this effect was not observed in the calculations performed using the conventional relativistic effective interaction [20]. Similar phenomenon was observed in the spin–isospin excitations of nuclei [39, 40, 47, 54]. This comparison indicates that strengths of the tensor force in the spin–isospin channel between the relativistic and non-relativistic effective interactions are different; this is because the relativistic one was constrained based only on the ground-state properties. As shown in Ref. [32], it is hard to determine the strength of the tensor force only by using the ground-state properties because central and spin–orbit interactions may also contribute to these differences. In fact, one can attain a good description of some ground-state properties, such as mass, even without including the tensor force [68, 69]; however, when dealing with single-particle energies [30, 31] or spin–isospin excitations [22, 42], the tensor force is essential because it provides a strong constraint for the tensor force [33, 43].

Author Contributions All authors contributed to the study conception and design. Material preparation, data collection, and analysis were performed by Da-Zhuang Chen, Dong-Liang Fang, and Chun-Lin Bai. The first draft of the manuscript was written by Da-Zhuang Chen, and all authors commented on previous versions of the manuscript. All authors read and approved the final manuscript.

References

1. E.M. Burbidge, G.R. Burbidge, W.A. Fowler et al., Synthesis of the elements in stars. Rev. Mod. Phys. **29**, 547 (1957). https://doi.org/10.1103/RevModPhys.29.547
2. J.J. Cowan, F.-K. Thielemann, J.W. Truran, The R-process and nucleochronology. Phys. Rep. **208**, 267 (1991). https://doi.org/10.1016/0370-1573(91)90070-3
3. H.-L. Liu, D.-D. Han, P. Ji et al., Reaction rate weighted multilayer nuclear reaction network. Chin. Phys. Lett. **37**, 112601 (2020). https://doi.org/10.1088/0256-307X/37/11/112601
4. M. Ji, C. Xu, Quantum anti-zeno effect in nuclear $\beta $ decay. Chin. Phys. Lett. **38**, 032301 (2021). https://doi.org/10.1088/0256-307X/38/3/032301
5. K. Takahashi, M. Yamada, Gross theory of nuclear β-decay. Prog. Theor. Phys. **41**, 1470 (1969). https://doi.org/10.1143/PTP.41.1470
6. T. Tachibana, M. Yamada, Y. Yoshida, Improvement of the gross theory of β-decay. II: one-particle strength function. Prog. Theor. Phys. **84**, 641 (1990). https://doi.org/10.1143/ptp/84.4.641
7. K. Langanke, G. Martínez-Pinedo, Shell-model calculations of stellar weak interaction rates: II. Weak rates for nuclei in the mass range $A = 45 - 61$ in supernovae environments. Nucl.

Phys. A **673**, 481 (2000). https://doi.org/10.1016/S0375-9474(00)00131-7

8. G. Martínez-Pinedo, K. Langanke, Shell-model half-lives for $N = 82$ nuclei and their implications for the r process. Phys. Rev. Lett. **83**, 4502 (1999). https://doi.org/10.1103/PhysRevLett.83.4502
9. J.J. Cuenca-García, G. Martínez-Pinedo, K. Langanke et al., Shell model half-lives for r-process $N = 82$ nuclei. Eur. Phys. J. A **34**, 99 (2007). https://doi.org/10.1140/epja/i2007-10477-3
10. T. Suzuki, T. Yoshida, T. Kajino et al., β decays of isotones with neutron magic number of $N = 126$ and r-process nucleosynthesis. Phys. Rev. C **85**, 015802 (2012). https://doi.org/10.1103/PhysRevC.85.015802
11. Q. Zhi, E. Caurier, J.J. Cuenca-García et al., Shell-model half-lives including first-forbidden contributions for r-process waiting-point nuclei. Phys. Rev. C **87**, 025803 (2013). https://doi.org/10.1103/PhysRevC.87.025803
12. J. Krumlinde, P. Möller, Calculation of Gamow–Teller β-strength functions in the rubidium region in the RPA approximation with Nilsson-model wave functions. Nucl. Phys. A **417**, 419 (1984). https://doi.org/10.1016/0375-9474(84)90406-8
13. P. Möller, J. Randrup, New developments in the calculation of β-strength functions. Nucl. Phys. A **514**, 1 (1990). https://doi.org/10.1016/0375-9474(90)90330-O
14. I.N. Borzov, S. Goriely, J.M. Pearson, Microscopic calculations of β-decay characteristics near the $A = 130 r$-process peak. Nucl. Phys. A **621**, 307 (1997). https://doi.org/10.1016/S0375-9474(97)00260-1
15. D.L. Fang, B.A. Brown, T. Suzuki, Investigating β-decay properties of spherical nuclei along the possible r-process path. Phys. Rev. C **88**, 034304 (2013). https://doi.org/10.1103/PhysRevC.88.034304
16. D.D. Ni, Z.Z. Ren, β-decay rates of neutron-rich Zr and Mo isotopes in the deformed quasiparticle random-phase approximation with realistic interactions. Phys. Rev. C **89**, 064320 (2014). https://doi.org/10.1103/PhysRevC.89.064320
17. D.D. Ni, Z.Z. Ren, β^+/EC decay rates of deformed neutron-deficient nuclei in the deformed QRPA with realistic interactions. Phys. Lett. B **744**, 22 (2015). https://doi.org/10.1016/j.physletb.2015.03.025
18. T. Nikšić, T. Marketin, D. Vretenar et al., β-decay rates of r-process nuclei in the relativistic quasiparticle random phase approximation. Phys. Rev. C **71**, 014308 (2005). https://doi.org/10.1103/PhysRevC.71.014308
19. T. Marketin, D. Vretenar, P. Ring, Calculation of β-decay rates in a relativistic model with momentum-dependent self-energies. Phys. Rev. C **75**, 024304 (2007). https://doi.org/10.1103/PhysRevC.75.024304
20. Z.M. Niu, Y.F. Niu, H.Z. Liang et al., β-decay half-lives of neutron-rich nuclei and matter flow in the r-process. Phys. Lett. B **723**, 172 (2013). https://doi.org/10.1016/j.physletb.2013.04.048
21. J. Engel, M. Bender, J. Dobaczewski et al., β decay rates of r-process waiting-point nuclei in a self-consistent approach. Phys. Rev. C **60**, 014302 (1999). https://doi.org/10.1103/PhysRevC.60.014302
22. F. Minato, C.L. Bai, Impact of tensor force on β decay of magic and semimagic nuclei. Phys. Rev. Lett. **110**, 122501 (2013). https://doi.org/10.1103/PhysRevLett.110.122501
23. M.T. Mustonen, J. Engel, Global description of β-decay in even-even nuclei with the axially-deformed Skyrme finite-amplitude method. Phys. Rev. C **93**, 014304 (2016). https://doi.org/10.1103/PhysRevC.93.014304
24. M. Martini, S. Peru, S. Goriely, Gamow–Teller strength in deformed nuclei within the self-consistent charge-exchange quasiparticle random-phase approximation with the Gogny force. Phys. Rev. C **89**, 044306 (2014). https://doi.org/10.1103/PhysRevC.89.044306
25. T. Otsuka, R. Fujimoto, Y. Utsuno et al., Magic numbers in exotic nuclei and spin–isospin properties of the NN interaction. Phys. Rev. Lett. **87**, 082502 (2001). https://doi.org/10.1103/PhysRevLett.87.082502
26. T. Otsuka, T. Suzuki, R. Fujimoto et al., Evolution of nuclear shells due to the tensor force. Phys. Rev. Lett. **95**, 232502 (2005). https://doi.org/10.1103/PhysRevLett.95.232502
27. T. Otsuka, T. Matsuo, D. Abe, Mean field with tensor force and shell structure of exotic nuclei. Phys. Rev. Lett. **97**, 162501 (2006). https://doi.org/10.1103/PhysRevLett.97.162501
28. B.A. Brown, T. Duguet, T. Otsuka et al., Tensor interaction contributions to single-particle energies. Phys. Rev. C **74**, 061303(R) (2006). https://doi.org/10.1103/PhysRevC.74.061303
29. M. Grasso, Z.Y. Ma, E. Khan et al., Evolution of the proton *sd* states in neutron-rich Ca isotopes. Phys. Rev. C **76**, 044319 (2007). https://doi.org/10.1103/PhysRevC.76.044319
30. G. Colò, H. Sagawa, S. Fracasso et al., Spin–orbit splitting and the tensor component of the Skyrme interaction. Phys. Lett. B **646**, 227 (2007). https://doi.org/10.1016/j.physletb.2007.01.033
31. D.M. Brink, F.L. Stancu, Evolution of nuclear shells with the Skyrme density dependent interaction. Phys. Rev. C **75**, 064311 (2007). https://doi.org/10.1103/PhysRevC.75.064311
32. T. Lesinski, M. Bender, K. Bennaceur et al., Tensor part of the Skyrme energy density functional: spherical nuclei. Phys. Rev. C **76**, 014312 (2007). https://doi.org/10.1103/PhysRevC.76.014312
33. D. Wu, C.-L. Bai, H. Sagawa et al., Contributions of optimized tensor interactions on the binding energyies. Nucl. Sci. Tech. **31**, 14 (2020). https://doi.org/10.1007/s41365-020-0727-7
34. E.B. Suckling, P.D. Stevenson, The effect of the tensor force on the predicted stability of superheavy nuclei. Europhys. Lett. **90**, 12001 (2010). https://doi.org/10.1209/0295-5075/90/12001
35. X.-R. Zhou, H. Sagawa, Effect of tensor interaction on heavy and superheavy nuclei. Mod. Phys. Lett. A **25**, 1809 (2010). https://doi.org/10.1142/S0217732310000381
36. L.-G. Cao, G. Colò, H. Sagawa et al., Effects of the tensor force on the multipole response in finite nuclei. Phys. Rev. C **80**, 064304 (2009). https://doi.org/10.1103/PhysRevC.80.064304
37. D. Davesne, M. Martini, K. Bennaceur et al., Nuclear response for the Skyrme effective interaction with zero-range tensor terms. Phys. Rev. C **80**, 024314 (2009). https://doi.org/10.1103/PhysRevC.80.024314
38. L.-G. Cao, H. Sagawa, G. Colò, Effects of tensor correlations on low-lying collective states in finite nuclei. Phys. Rev. C **83**, 034324 (2011). https://doi.org/10.1103/PhysRevC.83.034324
39. C.L. Bai, H. Sagawa, H.Q. Zhang et al., Effect of tensor correlations on Gamow–Teller states in ^{90}Zr and ^{208}Pb. Phys. Lett. B **675**, 28 (2009). https://doi.org/10.1016/j.physletb.2009.03.077
40. C.L. Bai, H.Q. Zhang, X.Z. Zhang et al., Quenching of Gamow–Teller strength due to tensor correlations in ^{90}Zr and ^{208}Pb. Phys. Rev. C **79**, 041301(R) (2009). https://doi.org/10.1103/PhysRevC.79.041301
41. C.L. Bai, H.Q. Zhang, X.Z. Zhang et al., Effect of the tensor force on charge-exchange spin-dependent multipole excitations. Chin. Phys. Lett. **27**, 102101 (2010). https://doi.org/10.1088/0256-307X/27/10/102101
42. C.L. Bai, H.Q. Zhang, H. Sagawa et al., Effect of the tensor force on the charge exchange spin-dipole excitations of ^{208}Pb. Phys. Rev. Lett. **105**, 072501 (2010). https://doi.org/10.1103/PhysRevLett.105.072501
43. C.L. Bai, H.Q. Zhang, H. Sagawa et al., Spin–isospin excitations as quantitative constraints for the tensor force. Phys. Rev. C **83**, 054316 (2011). https://doi.org/10.1103/PhysRevC.83.054316

44. L.J. Jiang, S. Yang, B.Y. Sun et al., Nuclear tensor interaction in a covariant energy density functional. Phys. Rev. C **91**, 034326 (2015). https://doi.org/10.1103/PhysRevC.91.034326
45. Z.-H. Wang, Q. Zhao, H.Z. Liang et al., Quantitative analysis of tensor effects in the relativistic Hartree–Fock theory. Phys. Rev. C **98**, 034313 (2018). https://doi.org/10.1103/PhysRevC.98.034313
46. J. Geng, J. Xiang, B.Y. Sun et al., Relativistic Hartree–Fock model for axially deformed nuclei. Phys. Rev. C **101**, 064302 (2020). https://doi.org/10.1103/PhysRevC.101.064302
47. T. Marketin, E. Litvinova, D. Vretenar et al., Fragmentation of spin-dipole strength in ^{90}Zr and ^{208}Pb. Phys. Lett. B **706**, 477 (2012). https://doi.org/10.1016/j.physletb.2011.11.050
48. H.Z. Liang, N.V. Giai, J. Meng, Spin–isospin resonances: a self-consistent covariant description. Phys. Rev. Lett. **101**, 122502 (2008). https://doi.org/10.1103/PhysRevLett.101.12250
49. Z.H. Wang, T. Naito, H.Z. Liang et al., Self-consistent random-phase approximation based on the relativistic Hartree–Fock theory: role of ρ-tensor coupling. Phys. Rev. C **101**, 064306 (2020). https://doi.org/10.1103/PhysRevC.101.064306
50. M. Anguiano, M. Grasso, G. Cò, V. De Donno et al., Tensor and tensor-isospin terms in the effective Gogny interaction. Phys. Rev. C **86**, 054302 (2012). https://doi.org/10.1103/PhysRevC.86.054302
51. M. Grasso, M. Anguiano, Tensor parameters in Skyrme and Gogny effective interactions: trends from a ground-state-focused study. Phys. Rev. C **88**, 054328 (2013). https://doi.org/10.1103/PhysRevC.88.054328
52. G. Cò, M. Anguiano, V. De Donno et al., Matter distribution and spin–orbit force in spherical nuclei. Phys. Rev. C **97**, 034313 (2018). https://doi.org/10.1103/PhysRevC.97.034313
53. M. Anguiano, G. Cò, V. De Donno, A.M. Lallena, Tensor effective interaction in self-consistent random-phase approximation calculations. Phys. Rev. C **83**, 064306 (2011). https://doi.org/10.1103/PhysRevC.83.064306
54. V. De Donno, G. Cò, M. Anguiano, A.M. Lallena, Charge-exchange excitations with finite-range interactions including tensor terms. Phys. Rev. C **90**, 024326 (2014). https://doi.org/10.1103/PhysRevC.90.024326
55. I.N. Borzov, S. Goriely, Weak interaction rates of neutron-rich nuclei and the r-process nucleosynthesis. Phys. Rev. C **62**, 035501 (2000). https://doi.org/10.1103/PhysRevC.62.035501
56. C. Gaarde, in *Proceedings of the Niels Bohr Centennial Conference*, edited by R. Broglia, G. Hagemann, and B. Herskind (North-Holland, Amsterdam, 1985), p. 449
57. E. Caurier, G. Martínez-Pinedo, F. Nowacki et al., The shell model as a unified view of nuclear structure. Rev. Mod. Phys. **77**, 427 (2005). https://doi.org/10.1103/RevModPhys.77.427
58. M. Kleban, B. Nerlo-Pomorska, J.F. Berger et al., Global properties of spherical nuclei obtained from Hartree–Fock–Bogoliubov calculations with the Gogny force. Phys. Rev. C **65**, 024309 (2002). https://doi.org/10.1103/PhysRevC.65.024309
59. J. Decharge, M. Girod, D. Gogny, Self consistent calculations and quadrupole moments of even Sm isotopes. Phys. Lett. B **55**, 361 (1975). https://doi.org/10.1016/0370-2693(75)90359-7
60. D. Gogny, in *Nuclear Self-Consistent Fields*, edited by G. Ripka, M. Porneuf (North-Holland, Amsterdam, 1975)
61. N. Onishi, J.W. Negele, Two-body and three-body effective interactions in nuclei. Nucl. Phys. A **301**, 336 (1978). https://doi.org/10.1016/0375-9474(78)90266-X
62. J.F. Berger, M. Girod, D. Gogny, Microscopic analysis of collective dynamics in low energy fission. Nucl. Phys. A **428**, 23 (1984). https://doi.org/10.1016/0375-9474(84)90240-9
63. S. Goriely, S. Hilaire, M. Girod et al., First Gogny–Hartree–Fock–Bogoliubov nuclear mass model. Phys. Rev. Lett. **102**, 242501 (2009). https://doi.org/10.1103/PhysRevLett.102.242501
64. M. Anguiano, A.M. Lallena, G. Cò, V. De Donno et al., Gogny interactions with tensor terms. Eur. Phys. J. A **52**, 183 (2016). https://doi.org/10.1140/epja/i2016-16183-1
65. P.D. Cottle, K.W. Kemper, Single-neutron energies near $N = 28$ and the absence of the $N = 34$ subshell closure in the Ti isotopes. Phys. Rev. C **78**, 037304 (2008). https://doi.org/10.1103/PhysRevC.78.037304
66. G. Audi, F.G. Kondev, M. Wang et al., The NUBASE2016 evaluation of nuclear properties. Chin. Phys. C **41**, 030001 (2017). https://doi.org/10.1088/1674-1137/41/3/030001
67. National Nuclear Data Center, "NuDat 2.8 Database"
68. S. Goriely, N. Chamel, J.M. Pearson, Further explorations of Skyrme–Hartree–Fock–Bogoliubov mass formulas. XIII. The 2012 atomic mass evaluation and the symmetry coefficient. Phys. Rev. C **88**, 024308 (2013). https://doi.org/10.1103/PhysRevC.88.024308
69. S. Goriely, N. Chamel, J.M. Pearson, Further explorations of Skyrme–Hartree–Fock–Bogoliubov mass formulas. XVI. Inclusion of self-energy effects in pairing. Phys. Rev. C **93**, 034337 (2016). https://doi.org/10.1103/PhysRevC.93.034337